Burn Rate Characterization of Red Iron Oxide Catalyst in Ammonium Perchlorate Composite Propellant

Connor M. Johnson* and Jaiden H. Patel†
Georgia Institute of Technology, Atlanta, GA, 30332

In solid rocket motor design, the burn rate of the propellant is a vital characteristic that influences the shape and magnitude of the resultant thrust curve. Motor internal ballistics is of interest to the Ramblin' Rocket Club's (RRC) experimental rocketry team, Georgia Tech Experimental Rocketry (GTXR). GTXR seeks to be the first collegiate team to send a two-stage sounding rocket to the Kármán line, a widely-recognized boundary of outer space. In service of this goal, the team seeks to develop a faster-burning propellant for use in higher-impulse motors. In this paper, burn rate sensitivity to chamber pressure is presented for a new ammonium perchlorate composite propellant (APCP) with a red iron oxide catalyst. The new propellant was developed by modifying GTXR's heritage formulation and mixing procedure to incorporate the catalyst before oxidizer addition. A reusable motor apparatus was designed and manufactured with nozzle inserts of different throat diameters to test a range of chamber pressures over multiple hot-fire tests. Pressure transducer data was used to generate a history of the burn for each hot-fire test, which was then split into transient and steady-state pressure regions. Steady-state burn rate was characterized according to St. Robert's Law, and these results were validated by studying the effect of motor contraction ratio in NASA's Chemical Equilibrium with Applications software. The empirically-derived burn rate coefficient a and exponent n suggest that the new propellant burns roughly 25 percent faster than GTXR's heritage formulation in the pressure region tested (200-800 psi). These results are further validated by comparison with reports from NASA and Rockwell International Corporation. The burn rate properties of the new formulation are being used to improve the performance of future solid rocket motors designed by GTXR.

I. Nomenclature

a	=	burn rate coefficient
A_b	=	exposed burn area
A^*	=	nozzle throat area
$APCP$	=	ammonium perchlorate composite propellant
c^*	=	characteristic velocity
$GTXR$	=	Georgia Tech Experimental Rocketry
K_n	=	restriction ratio
M_s	=	mass stored in chamber
n	=	pressure exponent
P_0	=	chamber pressure
r	=	burn rate
RRC	=	Ramblin' Rocket Club
ρ_p	=	propellant density
ρ_0	=	chamber density
SRM	=	solid rocket motor
v_0	=	chamber volume
γ	=	ratio of specific heats

*Undergraduate Student, Daniel Guggenheim School of Aerospace Engineering, Georgia Institute of Technology, 620 Cherry Street NW, Atlanta GA 30332, AIAA Student Member, 1325903

†Undergraduate Student, Daniel Guggenheim School of Aerospace Engineering, Georgia Institute of Technology, 620 Cherry Street NW, Atlanta GA 30332, AIAA Student Member, 1603540

$HTPB$ = Hydroxyl-terminated polybutadiene
$PBAN$ = Polybutadiene acrylonitrile

II. Introduction

The burn rate characterization of propellant for a solid rocket motor (SRM) plays a key role in predicting motor performance in a flight environment. Georgia Tech Experimental Rocketry (GTXR) is attempting to be the first collegiate team to send a two-stage sounding rocket to the Karman Line, the 100 km altitude marker which informally defines the edge of outer space. GTXR is a project team within the Ramblin' Rocket Club, a registered student organization at the Georgia Institute of Technology. Besides building and testing SRMs for the last four years, GTXR has also taken significant effort to predict motor performance through propellant characterization, the study of propellant properties during motor operation.

A key part of SRM propellant characterization relies on the relation between burn rate and chamber pressure. This relationship is unique to each solid propellant and is essential to know for the prediction of chamber pressure over time, which drives the thrust and trajectory of a vehicle.

Since its founding, GTXR has utilized an ammonium perchlorate composite propellant (APCP) formulation derived from the West Virginia University Experimental Rocketry Team. Internal simulations conducted by GTXR have suggested that increasing the burn rate of this propellant for larger motors could offer structural mass reductions or burn time reductions, both of which are optimal for building more efficient motors. To achieve this benefit in other contexts, hobbyists and engineers have used catalysts that are mixed into a baseline APCP formulation as a means of elevating the burn rate. This paper outlines the modelling, experimental setup, and results of adding a Iron(III) oxide (red iron oxide) catalyst into a heritage APCP formulation, led by the GTXR Propulsion Team in the Spring of 2023.

III. Solid Rocket Motor Internal Ballistics

Knowledge of the chamber pressure over time is among the most critical facets to SRM operation. A pressure vs. time curve generated by the motor governs thrust and vehicle trajectory, so it is of utmost importance to predict this curve in the design phase. A traditional SRM has three main phases of operation: transient start-up, steady state, and transient tail-off. Transient start-up is defined as the window of rapid pressurization during and shortly after ignition, where the flame spreads to all of the exposed burning surfaces on the grains. Steady-state operation is defined as the region of lowest pressure change post ignition, where the grain geometry itself controls pressure. Tail-off is defined as the window when grain consumption is nearing completion and chamber pressure falls back to ambient conditions. For the scope of this project, understanding the steady-state operation of the motor was chosen due to it being the largest time window in motor operation.

It is useful to develop a model for steady-state chamber pressure because it allows for the sizing of propellant grains to produce the desired thrust curve. The authors utilized the work of Richard Nakka [1], who developed a steady-state chamber pressure model by treating the motor interior as a control volume. In his model, the mass flow rate of combustion gasses generated by the propellant grain $\dot{m}_g$ is equal to the change in stored mass inside the chamber interior $\frac{dM_s}{dt}$ plus the mass flow rate of gasses leaving through the nozzle $\dot{m}_n$. Figure 1 displays a CV model of the motor used.

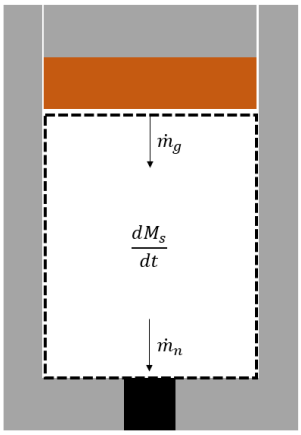

Fig. 1 Control volume analysis of a solid rocket motor.

Equation (1) describes the conservation of mass inside the motor, where $\dot{m}_g$ is also equal to the product of exposed burning area A_b, propellant density ρ_p, and burn rate r.

$$\dot{m}_g = \frac{dM_s}{dt} + \dot{m}_n = A_b \rho_p r \tag{1}$$

The rate of change in stored mass inside the CV with respect to time accounts for the change in CV density ρ_0 and volume v_0.

$$\frac{dM_s}{dt} = \frac{d}{dt}(\rho_0 v_0) = \rho_0 \frac{dv_0}{dt} + v_0 \frac{d\rho_0}{dt} \tag{2}$$

The change in v_0 with respect to time corresponds to the propellant volume changing at a rate of A_b times r.

$$\frac{dv_0}{dt} = A_b r \tag{3}$$

Plugging in Equation (3) into Equation (2) yields

$$\frac{dM_s}{dt} = \rho_0 A_b r + v_0 \frac{d\rho_0}{dt} \tag{4}$$

Plugging Equation (4) into (1) yields

$$A_b \rho_p r = \rho_0 A_b r + v_0 \frac{d\rho_0}{dt} + \dot{m}_n \tag{5}$$

Because the nozzle induces the choked flow condition, the mass flow rate leaving the motor through the nozzle is given by

$$\dot{m}_n = P_0 A^* \sqrt{\frac{\gamma}{RT_0}} \left(\frac{2}{\gamma+1}\right)^{\frac{\gamma+1}{2(\gamma-1)}} \tag{6}$$

Chamber pressure is closely linked to the burn rate of the solid rocket propellant, which is rate at which the propellant grain regresses in the direction normal to its surface. For many propellants, the relation between chamber pressure and burn rate has been observed to follow St. Robert's Law:

$$r = a P_0^n \tag{7}$$

The two constants a and n must be experimentally determined. The time derivative of ρ_0 can be found according to the ideal gas law.

$$\frac{d\rho_0}{dt} = \frac{1}{RT_0} \frac{dP_0}{dt} \tag{8}$$

Plugging in Equations 6, 7, and 8 into 5 results in a generalized chamber pressure formula during motor operation.

$$\frac{v_0}{RT_0} \frac{dP_0}{dt} = A_b a P_0^n (\rho_p - \rho_0) - P_0 A^* \sqrt{\frac{\gamma}{RT_0}} \left(\frac{2}{\gamma+1}\right)^{\frac{\gamma+1}{2(\gamma-1)}} \tag{9}$$

Considering that the contribution of chamber density is marginal compared to propellant density, we can neglect ρ_0. To arrive at a steady-state equation for chamber pressure, the time derivative of P_0 vanishes.

$$P_0 = \left(\frac{A_b}{A^*}\frac{a\rho_p}{\sqrt{\frac{\gamma}{RT_0}\left(\frac{2}{\gamma+1}\right)^{\frac{\gamma+1}{\gamma-1}}}}\right)^{\frac{1}{1-n}} \tag{10}$$

The denominator can be simplified in terms of characteristic velocity, a measure of the combustion efficiency of the motor.

$$c^* = \sqrt{\frac{RT_0}{\gamma}\left(\frac{\gamma+1}{2}\right)^{\frac{\gamma+1}{\gamma-1}}} \tag{11}$$

The authors arrived at the final expression for steady state chamber pressure.

$$P_0 = \left(\frac{A_b}{A^*}a\rho_p c^*\right)^{\frac{1}{1-n}} \tag{12}$$

Equations (7) and (12) served as the baseline for propellant characterization, where estimates of a and n were obtained for the new propellant.

IV. Experimental Setup

1. Reusable Motor

In order to characterize the propellant, a full motor assembly consisting of a casing, forward closure, and nozzle was designed and manufactured. Figure 2 shows the cross-section of the designed motor.

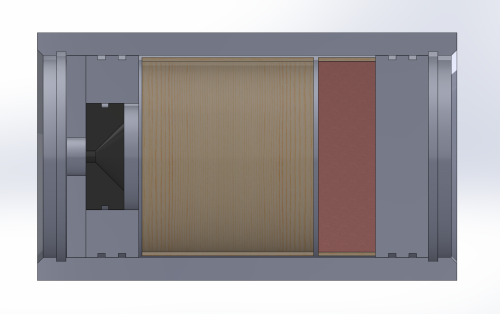

Fig. 2 Characterization Motor Assembly.

The forward closure and nozzle assembly were secured by steel internal retaining rings installed into casing grooves on either end. The nozzle assembly contains a small graphite insert at the throat. Multiple graphite inserts were machined with different throat diameters in order to reach different chamber pressures.

Due to the unpredictable nature of the propellant when initially tested, the motor hardware required a high factor of safety to minimize the probability of failure. All motor components were machined from Aluminum 6061, which has well-documented material strength conditions. The casing has a 5.29" inner diameter with a 0.5" wall thickness. The forward closure and nozzle carrier are 1.385" thick. An additional .25" thick plate retains the nozzle throat as seen in Figure 2. Based on thin-walled pressure vessel hand calculations, the motor has a minimum factor of safety of 6 at a chamber pressure of 1,000 psi. This was further validated with Finite Element Analysis.

The authors used 1" long end burning grains. Since exposed burn area on the aft circular face of the grain remains constant throughout the burn, the chamber pressure ideally remains constant in steady state. The nozzle throat diameters used for GT-ARES hot fire tests were significantly oversized based on GT-GOLD a and n values, ensuring that the motor will will not experience structural failure.

2. Propellants

The propellant development campaign tested a new APCP formulation, GT-ARES. GT-ARES is a derivative of GTXR's heritage formulation, GT-GOLD, whose burn rate characteristics had previously been characterized. Compared to GT-GOLD, GT-ARES contains 2 percent Iron(III) oxide (red iron oxide) by mass, and this addition replaced the equivalent mass of ammonium perchlorate in GT-GOLD. The red iron oxide was fully incorporated into the propellant mixture before the addition of ammonium perchlorate.

The casting tubes were cut to be a 1.5 inches long with a 5 inch ID and a 5.2 inch outer diameter. Using 3D-printed caps and bases, the propellant is mixed and packed into the casting tubes. After curing, the caps and bases are carefully removed and grains are post-processed down to have completely flat faces with a grain length of roughly 1". A coat of epoxy was applied to one face of the grain to inhibit propellant burning to only one side.

3. Test Stand

Because of the small size of the motor, the minimal thrust generated, and the overbuilt design of the motor, the authors designed a simplified test stand made of cinder blocks, steel components, and ratchet straps, as seen in Figure 3, saving time and resources.

Fig. 3 Characterization Motor Test Stand.

V. Results and Discussion

A series of hot fire tests of GTXR's baseline propellant, GT-GOLD, and the new experimental propellant, GT-ARES, were conducted using the experimental apparatus outlined above. Two hot fire tests of GT-GOLD were conducted to validate the instrumentation and internal ballistics model. Seven hot fire tests of GT-ARES were conducted, each at different nozzle diameters to induce a different chamber pressure according to Equation (12).

Fig. 4 GT-ARES Propellant Hot Fire Test.

A. Chamber Pressure Data

Figure 5 displays each pressure curve from the two hot fire tests of GT-GOLD.

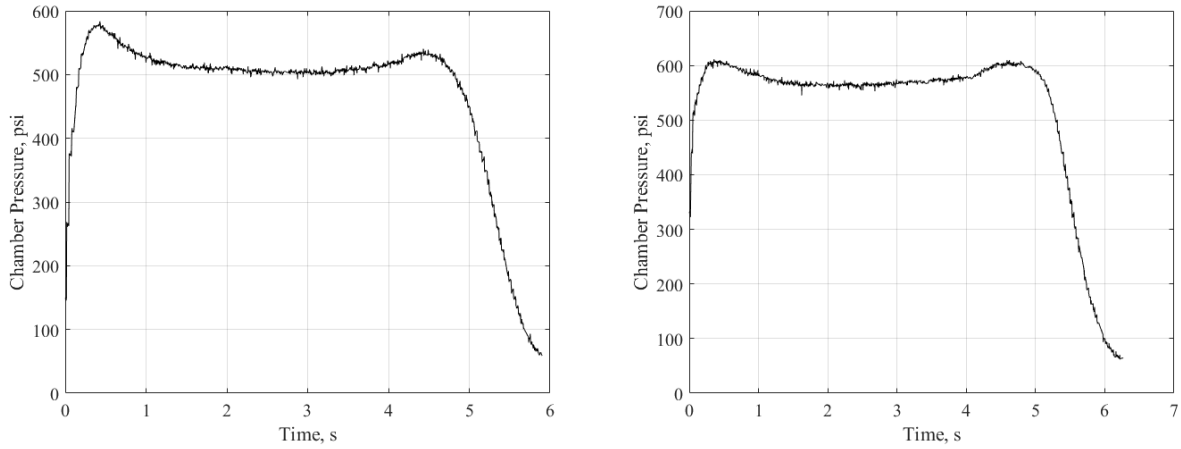

Fig. 5 GT-GOLD Hot Fire Pressure Curves.

Figure 6 displays each pressure curve from six hot fire tests of GT-ARES. Unfortunately, a malfunction in the Data Acquisition System during a hot fire test at 244 psi steady state chamber pressure prevented the formation of a pressure curve.

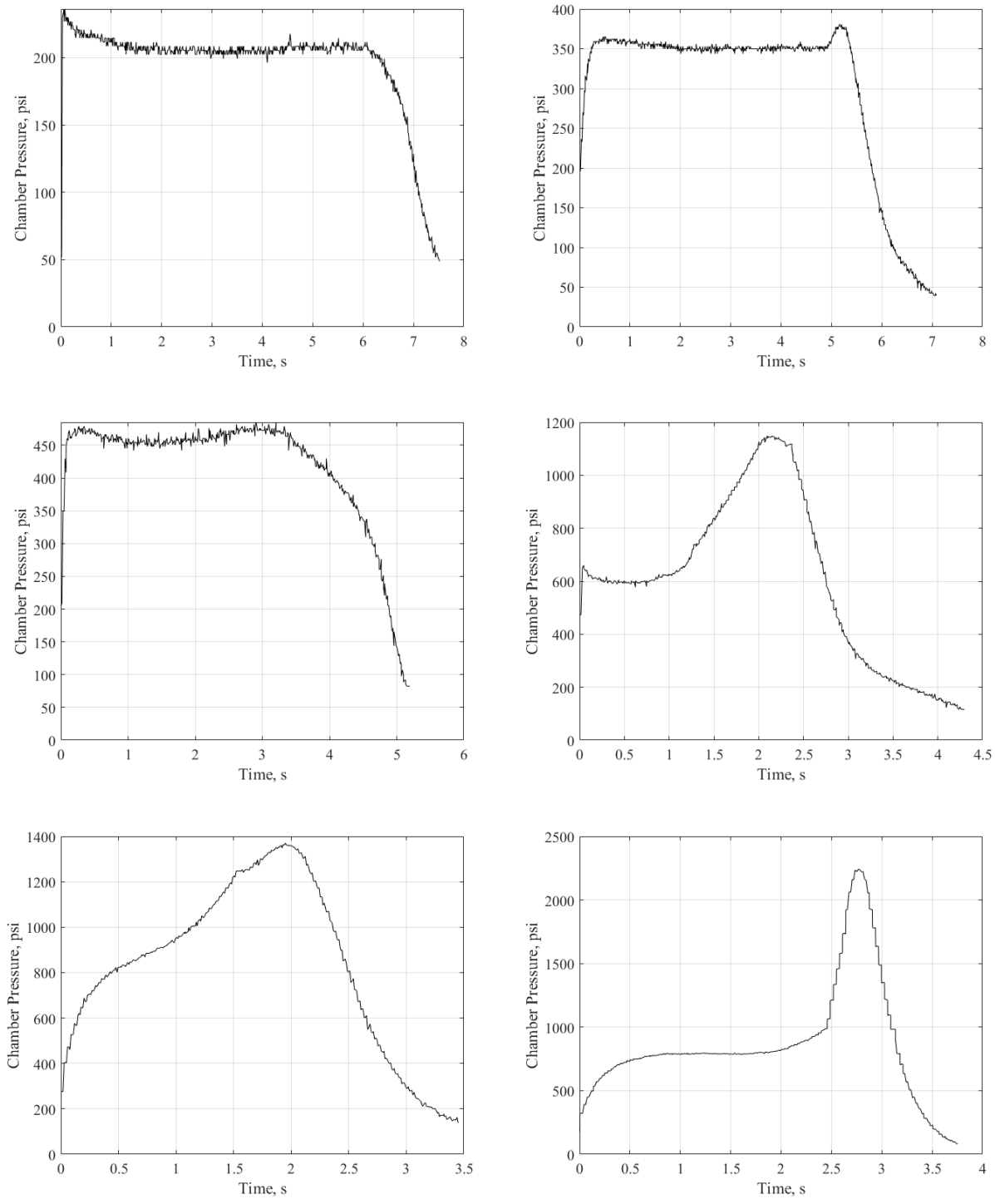

Fig. 6 GT-ARES Hot Fire Pressure Curves.

The following tables display the nozzle dimensions and pressure and burn rate data collected from each hot fire test. Note that burn rate was calculated by dividing the grain length by burn time in order to find an average value.

Table 1 GT-GOLD hot fire nozzle dimensions and testing data. The pressure in each neutral region is displayed in parenthesis.

Test	Nozzle Diameter (in)	Average Pressure (psi)	Grain Length (in)	Burn Time (s)	Burn Rate (in/s)
1	0.281	471 (510)	1	5.9053	0.1693
2	0.266	522 (570)	1	6.2674	0.1596

Table 2 GT-ARES hot fire nozzle dimensions and testing data. The pressure in each neutral region is displayed in parenthesis.

Test	Nozzle Diameter (in)	Average Pressure (psi)	Grain Length (in)	Burn Time (s)	Burn Rate (in/s)
1	0.406	196 (210)	1.1	7.5184	0.1463
2	0.375	N/A(244)	N/A	N/A	0.1572
3	0.344	300 (350)	1.15	7.0799	0.1624
4	0.328	418 (460)	1.1	5.1930	0.2118
5	0.313	599 (610)	1.1	4.2968	0.2560
6	0.281	831 (840)	1.1	3.4503	0.3188
7	0.281	855 (790)	1.31	3.7551	0.3489

B. Data Reduction

Although two hot fires were conducted for GT-GOLD, data reduction to find a and n was only conducted for GT-ARES. The hot fires for GT-GOLD served to validate the Data Acquisition System and the previously-determined a and n for the propellant.

1. Steady-State Prediction

Using Equation (12), knowledge of the burn area, throat area, and steady state chamber pressure can be used to determine a and n. This analysis is performed through knowledge of the restriction ratio, the ratio between burn area and nozzle throat area ($K_n = \frac{A_b}{A^*}$). This yields a new expression for steady state chamber pressure.

$$P_0 = (K_n a \rho_p c^*)^{\frac{1}{1-n}} \tag{13}$$

The burn area for each propellant grain is assumed to be constant in an end-burning configuration. By varying the throat area and identifying the neutral region of each pressure curve (neglecting anomalous spikes), a relation between steady-state chamber pressure and restriction ratio can be used to find a and n. With P_0 and K_n known from each hot fire, Equation 13 was fit according to a power series curve in order to solve for a and n. During propellant mixing, ρ_p was calculated by measuring the mass and volume of each grain. Characteristic velocity c^* was determined by inserting the propellant combustion properties into NASA Chemical Equilibrium with Applications in MATLAB (CEAM) [2]. Since c^* is independent of chamber pressure, the value was assumed to be constant across all hot fires.

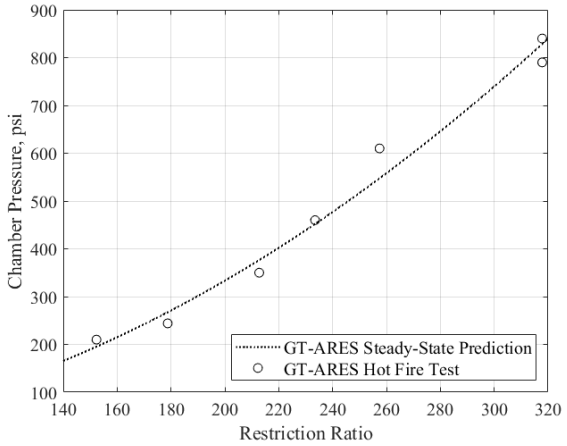

Fig. 7 GT-ARES steady-state chamber pressure response to restriction ratio.

2. Average Value Prediction

Average chamber pressures and average burn rates over the duration of each hot fire were obtained. Using Equation (7), these values were plotted and curve-fitted according to a power series to obtain experimental values for a and n.

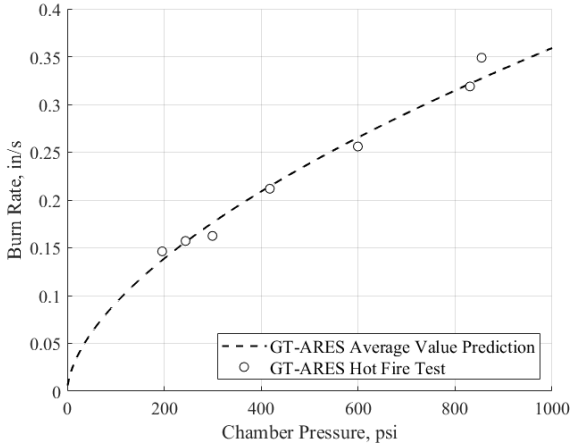

Fig. 8 GT-ARES average chamber pressure and burn rate data.

C. Summary of Empirical Burn Rate Constants

The a and n value extracted from the Steady-State and Average Value Predictions are shown below.

Table 3 GT-ARES empirically-determined burn rate constants.

Prediction Method	a	n	R^2
Steady-State	0.011	0.491	0.9816
Average Value	0.006	0.591	0.9778

In order to determine a final set of a and n for GT-ARES, the power series curves from both methods were averaged to produce a curve in the middle of both. Equal weight was given to each prediction method, given the high coefficients of determination for both. Next, the final St. Robert's Law curves for both GT-GOLD and GT-ARES are shown below.

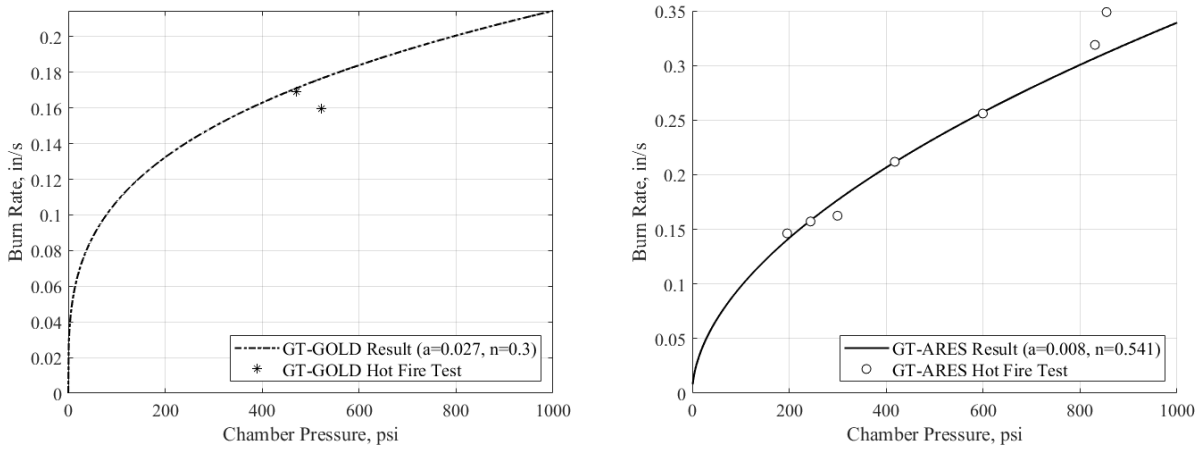

Fig. 9 Final GT-GOLD and GT-ARES Curve Fits.

Table 4 Empirically-determined burn rate constants.

Propellant	a	n
GT-GOLD	0.027	0.3
GT-ARES	0.008	0.541

Compared to GT-GOLD, GT-ARES has a lower a and higher n. This change indicates GT-ARES's greater burn rate sensitivity to chamber pressure as well as higher burn rates within the 200-1,000 psi range tested. The two GT-GOLD hot fires deviate from the heritage a and n, indicating that further study is needed to explain the deviation.

D. Pressure Anomalies

Upon disassembly of the motor after hot fires 5 and 6 for GT-ARES, which contained considerable pressure spikes, the authors observed that the casting tube holding the propellant had charred completely through the wall thickness and began to dislodge itself inside the motor. The authors believe that the flame might have spread to the opposite side of the propellant grain, nearly instantaneously increasing burn area and therefore chamber pressure. Similar evidence was found in hot fire 7. For future studies, the authors plan to employ a stronger, more flame-resistant epoxy to the inhibited side of the grain.

E. Verification of Results

1. Comparison to Existing Literature

Solid propellant burn rate augmentation has been a mature technology for the last half century. In 1971, Douglass [3] details how adding iron catalysts, including red iron oxide, to PBAN propellants boosts burn rates. Based on their experimental data, as catalyst level percentage is raised, burn rate heavily grows initially, but it begins to stabilize after reaching 2 percent. While PBAN propellant is not the same as the APCP base for GT-ARES propellant, this suggests that choosing a catalyst percentage of 2 percent for GT-ARES is a reasonable addition for developing a faster burning propellant without being too costly or significantly altering total composition of the propellant.

Burnside [4] also investigated (as part of a Rockwell report) the role of red iron oxide in propellant burn rate enhancement and documented the effects of the catalyst on the burn rate and pressure exponent. This test uses a 1 percent red iron oxide catalyst with different specific surfaces and details the resulting performance for HTPB propellants, which is what GT-ARES consists of. The burn rates in this study are overall significantly greater than the GT-ARES or GT-GOLD burn rates. However, this is likely due to a different propellant composition, specifically with the ammonium perchlorate particle sizes used. The difference between GT-GOLD and GT-ARES burn rates at 600 psi is roughly .1 in/s.

This is slightly less than the difference for Rockwell's smallest tested surface density, but the authors believe GT-ARES has a significantly smaller surface density, which would put the expected difference in burn rate within an acceptable margin.

Burnside also discusses their findings on the correlation between burn rate, specific surface, and coarse ammonium perchlorate particle size. As the particle size moves closer towards a balanced ratio between 200μ and 400μ, they also found that the burn rate is roughly between .4 to .5 in/sec, varying greatly by specific surface. The specific surface is not able to measured for GT-ARES, but as mentioned, the authors believe the specific surface is very small. By extrapolating the Rockwell data for a AP 400-200 micron blend, the burn rate tends towards a value between .3 and .4 in/sec. This Rockwell experiment was conducted at 1,000 psi. Based on the final curve fit, GT-ARES is expected to have a burn rate around 3.3 in/sec at 1,000 psi. This reasonably supports that GT-ARES is successfully characterized through the tested pressure range of 200-800 psi. However, by extrapolating using this data on Fig. 14 and accounting for the additional percentage of red iron oxide that GT-ARES uses, the pressure exponent for GT-ARES is roughly within an expected margin in the pressure range of 200-800 psi.

VI. Conclusion

With the addition of red iron oxide to the GT-GOLD propellant formula, the burn rate performance of GT-ARES was significantly elevated, especially at higher chamber pressures. The empirically determined a and n values from Table 4 result from high coefficients of determination, validating the steady-state and average value reduction methods. The results are further validated by experimental data from former studies that have demonstrated the burn rate elevation from addition of red iron oxide into APCP. This high degree of confidence suggests that the resulting curve fit accurately predicts the burn rate through the tested pressure region for end burner grains of GT-ARES. The next step is to test the propellants in cylindrical port grains for larger motors in order to characterize erosive burning augmentation to the burn rate. This knowledge will then allow GTXR to accurately simulate internal motor ballistics with both propellant formulations in pursuit of developing higher-performance solid rocket motors.

Acknowledgments

The authors thank the Student Government Association at Georgia Tech and the Daniel Guggenheim School of Aerospace Engineering for logistically and financially supporting the Ramblin' Rocket Club. The authors thank RRC's additional financial sponsors who contribute to the success of the team. Lastly, the authors also thank the members of the GTXR Propulsion Team for assistance in the design and manufacture of the reusable motor and in testing operations.

References

[1] Nakka, R., "Solid Rocket Motor Theory – Chamber Pressure," , 2001. URL https://www.nakka-rocketry.net/th_pres.html, cited 1 December 2023.

[2] NASA Marshall Space Flight Center, "Chemical Equilibrium with Applications in MATLAB (CEAM)," Version 1.0.0.0, 2017. Available: https://software.nasa.gov/software/MFS-33320-1.

[3] Douglass, H. W., "Solid Propellant Selection and Characterization," Tech. rep., NASA SP-8064, June 1971. URL https://ntrs.nasa.gov/api/citations/19720006088/downloads/19720006088.pdf.

[4] Burnside, C. H., "Role of Ferric Oxide Surface Area in Propellant Burn Rate Enhancement," Tech. rep., Rockwell International Corporation, June 1975. URL https://apps.dtic.mil/sti/pdfs/ADA013855.pdf.